



1 **Background Heterogeneity and Other Uncertainties in**
2 **Estimating Urban Methane Flux: Results from the**
3 **Indianapolis Flux (INFLUX) Experiment**
4

5 Nikolay V. Balashov¹, Kenneth J. Davis¹, Natasha L. Miles¹, Thomas Lauvaux^{1,2},
6 Scott J. Richardson¹, Zachary R. Barkley¹, Timothy A. Bonin^{3,4}

7
8 ¹The Pennsylvania State University, University Park, Pennsylvania, USA

9 ²Laboratory of Climate Sciences and Environment, Gif-sur-Yvette, France

10 ³Cooperative Institute for Research in Environmental Sciences, Boulder, Colorado, USA

11 ⁴Chemical Sciences Division, National Oceanic and Atmospheric Administration, Boulder, Colorado,
12 USA

13

14 **Abstract**

15 As natural gas extraction and use continues to increase, the need to quantify emissions of methane
16 (CH₄), a powerful greenhouse gas, has grown. Large discrepancies in Indianapolis CH₄ emissions
17 have been observed when comparing inventory, aircraft mass-balance, and tower inverse modeling
18 estimates. Four years of continuous CH₄ mole fraction observations from a network of nine tower-
19 based cavity ring-down spectrometers measuring atmospheric CH₄ mole fractions at 39 to 136 m
20 above ground as part of the Indianapolis Flux Experiment (INFLUX) are utilized to investigate
21 four possible reasons for the abovementioned inconsistencies: (1) differences in definition of the
22 city domain, (2) a highly temporally variable and spatially non-uniform CH₄ background, (3)
23 temporal variability in CH₄ emissions, and (4) the presence of unknown CH₄ sources. Reducing
24 the Indianapolis urban domain size to be consistent with the inventory domain size decreases the
25 CH₄ emission estimation of the inverse modeling methodology by about 35% and thereby lessens
26 the discrepancy by bringing total city flux within an error range of one of the inventories.
27 Nevertheless, the inverse modeling estimate still remains about 40% higher than the inventory
28 value. Hourly urban background CH₄ mole fractions are shown to be heterogeneous and
29 temporally variable. Statistically significant, long-term biases in background mole fractions of 2-



30 5 ppb are found from single point observations from most wind directions. Random errors in
31 single point background mole fractions observed for a few hours are 20-30 ppb, but decrease
32 substantially when data are averaged over multiple days. Boundary layer budget estimates suggest
33 that Indianapolis CH₄ emissions did not change significantly when comparing 2014 to 2016.
34 However, it appears that CH₄ emissions may follow a diurnal cycle with daytime emissions (12-
35 16 LST) approximately twice as large as nighttime emissions (20-5 LST). The strongest CH₄
36 source in Indianapolis is the South Side Landfill. Other point sources, perhaps leaks from the
37 natural gas distribution system, are localized and transient, and do not appear to be a consistently
38 large source of CH₄ emissions in Indianapolis. Long-term averaging, spatially-extensive upwind
39 mole fraction observations, mesoscale atmospheric modeling of the regional emissions
40 environment, and careful treatment of the times of day and areal representation of emission
41 estimates is recommended for precise and accurate quantification of urban CH₄ emissions.

42

43 **1 Introduction**

44 From the beginning of the Industrial Revolution to 2011, atmospheric methane (CH₄) mole
45 fractions increased by a factor of 2.5 due to anthropogenic processes such as fossil fuel production,
46 waste management, and agricultural activities (Ciais et al., 2013). The increase in CH₄ is a concern
47 as it is a potent greenhouse gas (GHG) with a global warming potential 28-34 times greater than
48 that of CO₂ over a period of 100 years (Myhre et al., 2013). The magnitudes of component CH₄
49 sources, and the causes of variability in the global CH₄ budget, however, are not well understood
50 although there is some evidence that biogenic emissions may play an important role in the recent
51 CH₄ increases (Nisbet et al., 2016; Saunio et al., 2016). Improved understanding of CH₄
52 emissions is needed (National Academies of Sciences and Medicine, 2018).



53 In particular, the estimates of continental U.S. anthropogenic CH₄ emissions disagree.
54 Inventories from Environment Protection Agency (EPA) and Emissions Database for Global
55 Atmospheric Research (EDGAR) in 2008 reported emission values of 19.6 and 22.1 TgC y⁻¹
56 (Miller et al., 2013). However, top-down methodologies using aircraft and inverse modeling
57 framework found emission values of 32.4 ± 4.5 TgC y⁻¹ for 2004 and 33.4 ± 1.4 TgC y⁻¹ for 2007-
58 2008 respectively (Kort et al., 2008; Miller et al., 2013). Underestimation of natural gas (NG)
59 production and agricultural sources are possible reasons for this disagreement (Miller et al., 2013;
60 Brandt et al., 2014; Jeong et al., 2014). Efforts to reconcile GHGs emissions estimates using
61 atmospheric methods and inventory assessment have succeeded (Schuh et al., 2013; Zavala-Araiza
62 et al., 2015; Turnbull et al., 2019) when careful attention is given to the details of each method,
63 and targeted atmospheric data are available. A recent synthesis of emissions from the U.S. NG
64 supply chain demonstrated similar success and concluded that current inventory estimates of
65 emissions from U.S. NG production are too low and that emission from NG distribution is one of
66 the greatest remaining sources of uncertainty in the natural gas supply chain (Alvarez et al., 2018).

67 Due to the uncertainties in CH₄ emissions from NG distribution it is natural that urban
68 emissions are of interest as well. For example, studies indicate that ~60-100% of Boston CH₄
69 emissions are attributable to the NG distribution system (McKain et al., 2015; Hendrick et al.,
70 2016). Recent studies of urban CH₄ emissions indicate that the California Air Resources Board
71 (CARB) inventory tends to underestimate the actual CH₄ urban fluxes possibly due to fugitive
72 emissions that result from the large NG infrastructures common to the urban environments (Wunch
73 et al., 2009; Jeong et al., 2016; Jeong et al., 2017). The accuracy and precision of atmospheric
74 estimates of urban CH₄ emissions are limited by available atmospheric observations (Townsend-
75 Small et al., 2012), potential source magnitude variability with time (Jackson et al., 2014; Lamb



76 et al., 2016), errors in atmospheric transport modeling (Hendrick et al., 2016; Deng et al., 2017;
77 Sarmiento et al., 2017;), and complexity in atmospheric background conditions (Cambaliza et al.,
78 2014; Heimburger et al., 2017). In this work, detailed analysis of urban CH₄ mole fractions is
79 performed in the city of Indianapolis to better understand the aforementioned uncertainties of
80 urban CH₄ emissions.

81 The Indianapolis Flux Experiment (INFLUX; Davis et al., 2017) is a testbed for improving
82 quantification of urban GHGs emissions and their variability in space and time. INFLUX
83 (<http://influx.psu.edu>) is located in Indianapolis partly because of its isolation from other urban
84 centers and the flat Midwestern terrain. It includes a very dense GHGs monitoring network,
85 comprised of in situ aircraft measurements (Heimburger et al., 2017; Cambaliza et al., 2014), in
86 situ observations from communications towers using cavity ring-down spectroscopy (Richardson
87 et al., 2017; Miles et al., 2017), and automated flask sampling systems for quantification of a wide
88 variety of trace gases (Turnbull et al., 2015). Meteorological sensors include a Doppler lidar
89 providing continuous boundary layer depth and wind profiles, and tower-based eddy covariance
90 measurements of the fluxes of momentum, sensible and latent heat (Sarmiento et al., 2017). The
91 network is well suited for emissions estimates using top-down methods such as tower-based
92 inverse modeling (Lauvaux et al., 2016) and aircraft mass balance estimates (Cambaliza et al.,
93 2015).

94 Recently Lamb et al. (2016) compared Indianapolis CH₄ emissions estimates from
95 inventory, aircraft mass balances, and inverse modeling. The results revealed large mean
96 differences among the city fluxes estimated from these methods (Fig. 1). In general, the inventory
97 methods arrived at lower estimates of emissions compared to the atmospheric, or top-down
98 approaches. CH₄ fluxes calculated using the aircraft mass balance technique varied considerably



99 between flights, more than would be expected from propagation of errors of the component
100 measurements (Cambaliza et al., 2014; Lamb et al., 2016). The atmospheric inverse estimate was
101 significantly higher than the inventory and some of the aircraft-derived values.

102 Biogenic emissions from the city are dominated by a landfill close to downtown, and these
103 emissions are thought to be fairly well known. Uncertainty in emissions is driven by the
104 uncertainty in thermogenic emissions, which are hypothesized to emerge largely from the NG
105 distribution system (Mays et al., 2009; Cambaliza et al., 2015; Lamb et al., 2016). This uncertainty
106 has not yet been resolved. In this study, we explore potential explanations for the discrepancies in
107 CH₄ emissions estimates from Indianapolis and posit methods and recommendations for the study
108 of CH₄ emissions from other urban centers.

109 We examine four different potential explanations for the CH₄ flux discrepancies reported
110 in Lamb et al. (2016): (1) inconsistent geographic boundaries, (2) heterogeneity in the urban-scale
111 CH₄ background, (3) temporal variability in urban emissions, and (4) CH₄ sources that are not
112 accounted for in the inventories. Well-calibrated CH₄ sensors on the INFLUX tower network
113 (Miles et al., 2017) collected continuous CH₄ observations from 2013 to 2016 and provide a unique
114 opportunity to explore these issues.

115

116 **2 Methods**

117

118 **2.1 Experimental site**

119 This study uses data from a tower-based GHG observational network located in the city and
120 surrounding suburbs of Indianapolis, Indiana, in the Midwestern U.S. Prior studies have used
121 varying definitions for the region of Indianapolis (Cambaliza et al., 2015, Lamb et al., 2016). In



122 this work, we follow Gurney et al. (2012) and define Indianapolis as the area of Marion County.
123 The flat terrain of the region simplifies interpretation of the atmospheric transport. The land-
124 surface heterogeneity inherent in the urban environment (building roughness, spatial variations in
125 the surface energy balance) do have a modest influence on the flow within the city and the
126 boundary layer depth difference between the urban and rural areas (Sarmiento et al., 2017).

127

128 **2.2 INFLUX tower network**

129 The continuous GHG measurements from INFLUX are described in detail in Richardson et al.
130 (2017). The measurements were made using wavelength-scanned cavity ring down spectrometers
131 (CRDS, Picarro, Inc., models G2301, G2302, G2401, and G1301), installed at the base of existing
132 communications towers, with sampling tubes secured as high as possible on each tower (39 – 136
133 m above ground level (AGL), Miles et al., (2017)). A few towers also included measurements at
134 10 m AGL and one or two intermediate levels. While INFLUX tower in-situ measurements began
135 in September 2010, here we focus on the CH₄ measurements from 2013 – 2016. From June
136 through December 2012, there were two or three towers with operational CH₄ measurements. By
137 July 2013, five towers included measurements of CH₄, and throughout the majority of the years
138 2015 – 2016 there were eight INFLUX towers with CH₄ measurements (Fig. 2).

139 By May 2013, the inflow to all CRDS instruments was dried. Prior to deployment and
140 following any manufacturer repairs, the instruments were calibrated for slope and offset in the
141 Pennsylvania State University calibration laboratory (Richardson et al., 2017) using three to five
142 NOAA-calibrated tanks. At each site, one or two NOAA-calibrated tanks were sampled daily for
143 10 min as field offset calibration points. In this study we used hourly means of CH₄, which were



144 reported on the WMO X2004A scale. Flask to in-situ comparisons and round-robin style testing
145 indicated compatibility across the tower network of 0.6 ppb CH₄ (Richardson et al., 2017).

146

147 **2.3 Weather data**

148 Wind data was measured at the Indianapolis International Airport (KIND), Eagle Creek Airpark
149 (KEYE), and Shelbyville Municipal Airport (KGEZ). The data used are hourly values from the
150 Integrated Surface Dataset (ISD) (<https://www.ncdc.noaa.gov/isd>) and 5-minute values directly
151 from the Automated Surface Observing System (ASOS). A complete description of ASOS stations
152 is available at <http://www.nws.noaa.gov/asos/pdfs/aum-toc.pdf>. The accuracy of the wind speed
153 is ± 1 m/s or 5% (whichever is greater) and the accuracy of the wind direction is 5 degrees when
154 the wind speed is ≥ 2.6 m/s. The anemometer is located about 10 meters AGL. The wind data
155 reported in ISD are given for a single point in time recorded within the last 10 minutes of an hour
156 and are closest to the value at the top of the hour.

157 The planetary boundary layer height (BLH) was determined from a Doppler lidar deployed
158 in Lawrence, IN, about 15 km to the northeast of downtown. The lidar is a Halo Streamline unit,
159 which was upgraded to have extended range capabilities in January 2016. The lidar continuously
160 performs a sequence of conical, vertical-slice, and staring scans to measure profiles of the mean
161 wind, turbulence, and relative aerosol backscatter. All of these measurements are combined using
162 a fuzzy-logic technique to automatically determine the BLH continuously every 20-min (Bonin et
163 al., 2018). The BLH is primarily determined from the turbulence measurements, but the wind and
164 aerosol profiles are also used to refine the BLH estimate. The BLHs are assigned quality-control
165 flags that can be used to identify times when the BLH is unreliable, such as when the air is
166 exceptionally clean, the BLH is below a minimum detectable height, or clouds and fog that



167 attenuate the lidar signal exist. Additional details about the algorithm and the lidar operation for
168 the INFLUX project are provided in Bonin et al. (2018). Doppler lidar measurements are available
169 at <https://www.esrl.noaa.gov/csd/projects/influx/>.

170

171 **2.4 CH₄ Sources**

172 Only a few known CH₄ point sources exist within Indianapolis (Cambaliza et al., 2015, Lamb et
173 al., 2016). The Southside Landfill (SSLF), located near the center of the city, is the largest point
174 source in the city with emissions of about 28-45 mol/s, accounting for 22% to 63% of total Marion
175 County CH₄ emissions (Cambaliza et al., 2015; Maasakkers et al., 2016; Lamb et al., 2016). Other
176 city point sources are comparatively small; the wastewater treatment facility located near SSLF
177 contributes approximately 4-10% to city CH₄ totals or about 3-7 mol/s, and the transmission-
178 distribution transfer station at Panhandle Eastern Pipeline (also known as a city gate and further in
179 this study abbreviated as PEP) is estimated to be about 0.5-1% or 1 mol/s. The remaining CH₄
180 sources, mainly from NG and livestock, are considered to be diffuse sources and are not well
181 known. Potential sources of emissions related to NG activities include gas regulation meters,
182 emissions from transmission and storage, and Compressed Natural Gas (CNG) fleets. These
183 diffuse NG sources account for 21-69% or 20-64 mol/s of the city emissions (Cambaliza et al.,
184 2015; Maasakkers et. al. 2016; Lamb et al., 2016). Livestock emissions for Marion County are
185 estimated to be around 3% or 1.5 mol/s.

186

187 **2.4 Urban methane background**

188 Both aircraft mass balance and inverse modeling methodologies rely on the accurate estimation of
189 the urban CH₄ enhancement relative to the urban CH₄ background in order to produce a reliable



190 flux estimate (Cambaliza et al., 2014; Lamb et al., 2016). The CH₄ mole fraction enhancement is
191 defined as,

$$C_{enhancement} = C_{downwind} - C_{bg} \quad (1)$$

192 where $C_{downwind}$ is the CH₄ mole fraction measured downwind of the source and C_{bg} is the CH₄
193 background mole fraction, which can be measured upwind of the source, but this is not necessary.
194 Background, as defined in this body of literature, is a mole fraction measurement that does not
195 contain the influence of the source of interest, but which is measured simultaneously. Because
196 choosing the background involves a degree of subjectivity (Cambaliza et al., 2014; Heimburger et
197 al., 2017) we consider how this choice may influence emission estimates and introduce error, both
198 random and systematic, using data from the INFLUX tower network.

199 Using tower network data from November, 2014 through the end of 2016, two CH₄
200 backgrounds are generated based on two different criteria. Both criteria identify a tower suitable
201 to serve as a background for each of the eight wind directions (N, NE, E, SE, S, SW, W, NW),
202 where an arc of 45° represents a direction (e.g. winds from N are between 337.5° and 22.5°).

203 Criterion 1 is based on the concept that the lowest CH₄ mole fraction measured at any given
204 time is not affected by the city sources and therefore is a viable approximation of the background
205 methane mole fractions outside of the city (Miles et al., 2017; Lauvaux et al., 2016). Given this
206 assumption, the tower with the lowest median of the CH₄ enhancement distribution (calculated by
207 assuming the lowest measurement among all towers at a given hour as a background) for each of
208 the wind directions over the November, 2014 through December, 2016 time period is chosen as a
209 background site (Miles et al., 2017). Criterion 2 requires that the tower is outside of Marion
210 County (outside of the city boundaries) and is not downwind of any known regional CH₄ source
211 (Fig. 3). For some wind directions, there are multiple towers that could qualify as a background;



212 we pick towers in such a manner that they are different for each criterion given a wind direction
213 in order to calculate the error associated with the use of different but acceptable backgrounds. The
214 towers used for both criteria and for each of the eight wind directions are displayed in Table 1.
215 Quantifying differences between these two backgrounds allows for an opportunity to better
216 understand the degree of uncertainty that exists in the Indianapolis background atmosphere.

217

218 **2.5 Frequency and bivariate polar plots**

219 Frequency and bivariate polar plots are used in this work to gain more knowledge regarding CH₄
220 background variability based on criteria 1 and 2, and to identify sources located within the city.
221 To generate these polar plots, we use the *openair* package (from R programming language) created
222 specifically for air quality data analysis (Carslaw and Ropkins, 2012). Bivariate and frequency
223 polar plots indicate the variability of a pollutant concentration at a receptor (such as an
224 observational tower) as a function of wind speed and wind direction, preferably measured at the
225 location of the receptor or within several kilometers of the receptor. The frequency polar plot is
226 generated by partitioning the CH₄ hourly data into the wind speed and direction bins of 1 m s⁻¹ and
227 10° respectively. To generate bivariate polar plots, wind components *u* and *v* are calculated for
228 hourly CH₄ concentration values, which are fitted to a surface using a Generalized Additive Model
229 (GAM) framework in the following way,

$$\sqrt{C} = \beta + s(u, v) + \epsilon \quad (2)$$

230 where *C* is the CH₄ mole fraction transformed by a square root to improve model diagnostics such
231 as a distribution of residuals, β is mean of the response, *s* is the isotropic smoothing function of
232 the wind components *u* and *v*, and ϵ is the residual. For more details on the model see Carslaw
233 and Beevers (2013).



234

235 **2.6 Temporal Variability**

236 Temporal variability may play an important role in the quantification of urban methane emissions.
237 Lamb et al., (2016) suggested that temporal variability may partially explain the differences among
238 CH₄ flux estimates shown in Fig. 1. If temporal variability of CH₄ emissions exists within the city,
239 disagreements in the CH₄ flux between studies could be attributed to differences in their sampling
240 period. Because the INFLUX tower data at Indianapolis contain measurements at all hours of the
241 day over multiple years, we can utilize this dataset to better understand the temporal variability in
242 methane emissions in the city.

243 We apply a simplified atmospheric boundary layer budget, not to estimate precisely the
244 actual city emissions, but rather to evaluate temporal variability of the emissions. We begin by
245 assuming CH₄ emissions Q_a (mass per unit time per unit area) are not chemically active and are
246 constant over a distance Δx spanning a significant portion of the city. The next assumption is that
247 a CH₄ plume measured upwind of the city is well mixed within a layer of depth z_i . We treat wind
248 speed u as constant within the layer for every hour considered. Given the above-mentioned
249 assumptions we can write a continuity equation describing mass conservation of CH₄
250 concentration C within a box in the following fashion,

$$\Delta x z_i \frac{\partial C}{\partial t} = \Delta x Q_a + u z_i (C_b - C) + \Delta x \frac{\partial z_i}{\partial t} (C_a - C) \quad (3)$$

251 where C_b is the CH₄ mole fraction upwind of the city (or background), and C_a is the CH₄
252 concentration above the mixed layer (Hanna et al., 1982; Arya, 1999; Hiller et al., 2014). The left
253 hand of the equation represents the change in CH₄ concentration with time, $\Delta x Q_a$ denotes a
254 constant CH₄ source over the distance Δx , $u z_i (C_b - C)$ indicates a change of CH₄ concentration
255 due to horizontal advection, and finally $\Delta x \frac{\partial z_i}{\partial t} (C_a - C)$ term accounts for the vertical advection



256 and encroachment processes that result from changing mixed layer height. By assuming steady
257 state conditions ($\frac{\partial C}{\partial t} = 0$ and $\frac{\partial z_i}{\partial t} = 0$), the equation can be simplified to

$$Q_a = \frac{uz_i(C - C_b)}{\Delta x} \quad (4)$$

258 We use equation 4 to estimate hourly CH₄ emissions (Q_a) from Indianapolis (see
259 assumptions in the paragraph below), given hourly data of z_i from the lidar positioned in the city,
260 wind speed from the local weather stations, and upwind (C_b) and downwind (C) CH₄
261 concentrations measured at towers 1, 8, and 13 (depending on wind direction) using data from
262 heights of 40 m, 41 m, and 87 m respectively (see Fig. 3).

263 The CH₄ concentrations are derived from CH₄ mole fractions by approximating average
264 molar density of dry air (in mol m⁻³) within the boundary layer for every hour of the day, where
265 variability of pressure with altitude is calculated using barometric formula and it is assumed that
266 temperature decreases with altitude by 6.5 K per kilometer. The hourly surface data for pressure
267 and temperature is taken from KIND weather station. The difference between concentrations
268 ($C - C_b$) is instantaneous and not lagged, where C_b represents air parcel entering the city and C
269 represents the same air parcel exiting the city (for more details see Turnbull et al., 2015). The CH₄
270 enhancements ($C - C_b$) are estimated for daytime by averaging observations spanning 12-16 LST
271 and for nighttime by averaging observations spanning 20-5 LST. These time periods are based on
272 lidar estimations of when on average z_i varies the least. The day and night were required to contain
273 at least 3 and 9 hourly CH₄ values respectively for averaging to occur, otherwise the day/night is
274 eliminated. Observations when z_i is below 100 m are not used to avoid the cases when
275 measurements from towers may be above the boundary layer. In order to better achieve the
276 assumption that the boundary layer is fully mixed (especially at night), all hours with wind speeds
277 below 4 m/s are eliminated (Van De Wiel., 2012). To approximate the emissions of the whole city



278 we need to know the approximate area of the city and the distance over which the plume is affected
279 by the city CH₄ sources. The area of the city is about 1024 km² (the area of Marion County) and
280 the length that plume traverses when it is over the city ranges from 32 to 35 km depending on
281 which downwind tower is used. We assume that CH₄ measurements at towers 8 and 13 are
282 representative of a vertically well-mixed city plume as the towers are located outside of the city
283 boundaries and allow for sufficient vertical mixing to occur. For S and SW wind directions tower
284 8 observations are used to represent downwind conditions with background observations coming
285 from towers 1 and 13, respectively (based on Criterion 1 shown in Table 1). For W wind direction,
286 tower 13 observations represent the downwind with background obtained from tower 1. The wind
287 direction is required to be sustained for at least 2 hours, otherwise the data point is eliminated.

288

289 **3 Results and discussion**

290

291 **3.1 City Boundaries**

292 A significant portion of CH₄ emissions across the U.S. can be characterized by numerous large
293 point sources scattered throughout the country rather than by broad areas of smaller enhancements
294 (Maasakkers et al., 2016). Because of this, the total emissions for a given domain can be very
295 sensitive to how that domain is defined. A small increase or a decrease in the domain area could
296 add or remove a large point source and significantly impact the total emissions defined within the
297 domain. This issue can be observed in prior studies of CH₄ emissions in Indianapolis, described
298 below.

299 In Fig. 3, two possible domains are identified (Lamb et al., 2016; Lauvaux et al., 2016) that
300 could be used for the evaluation of Indianapolis CH₄ emissions. The first domain is the whole area
301 shown in the figure enclosing both Indianapolis and places that lie outside of its boundaries. The
302 second domain is Marion County outlined with a green dashed line. It is assumed here that this



303 domain is much more representative of the actual Indianapolis municipal boundaries as this area
304 encompasses the majority of the urban development associated with the city of Indianapolis
305 (Gurney et al., 2012). The larger domain has three additional landfills that, based on the EPA
306 gridded inventory (Maasackers et al., 2016), increase CH₄ emissions by about 50% when
307 compared to the smaller domain.

308 This issue became apparent when the emissions were calculated using an atmospheric
309 inversion model (Lamb et al., 2016; Lauvaux et al., 2016). The atmospheric inversion solved for
310 fluxes in domain 1, which significantly increased the estimated emissions in comparison with the
311 inventory values that were gathered mainly within Marion County (domain 2). When reduced to
312 domain 2, inverse modeling emission estimates decrease to 107 mol/s, which falls within an error
313 bar of Lamb et al. (2016) inventory estimate. This difference is significant and could at least
314 partially explain the discrepancy shown in Fig. 1 between the emission values from the inventories
315 and emission results from the inverse modeling. However, even the decreased inverse modeling
316 estimate is about 40% higher than the inventory.

317 The subject of the domain is also relevant for airborne mass balance flights because a priori
318 the magnitude and variability of background plume is unknown and could be easily influenced by
319 upwind sources. The issue of background is discussed further in the next section.

320

321 **3.2 Variability in Background Tower Mole Fraction**

322 Comparisons between Criterion 1 and Criterion 2 CH₄ mole fraction enhancements as a
323 function of wind direction are visualized using frequency and bivariate polar plots (Fig. 4). To
324 make the comparison as uniform as possible, only data from 12-16 LST are utilized (all hours are
325 inclusive), when the boundary layer is typically well-mixed (Bakwin et al., 1998). A lag 1



326 autocorrelation is found between 12-16 LST hours, i.e., the hourly afternoon data are correlated to
327 the next hour, but the correlation is not significant for samples separated by two hours or more.
328 Therefore, hours 13 and 15 LST are eliminated to satisfy the independence assumption for hourly
329 samples. Furthermore, we make an assumption that the data satisfy steady state conditions. If the
330 difference between consecutive hourly wind directions exceeds 30 degrees or the difference
331 between hours 16 and 12 LST exceeds 40 degrees, the day is eliminated. Days with average wind
332 speeds below 2 m/s are also eliminated due to slow transport (the transit time from tower 1 to
333 tower 8 is about 7 hours at a wind speed of 2 m/s).

334 Both backgrounds generally agree on the higher CH₄ originating from the SW, SE, and E
335 wind directions (Figs. 4c-f); however, the values themselves differ especially when winds are from
336 NW, SW, and SE. As the background difference plots indicate, there is noticeable variability in
337 the magnitudes of the CH₄ mole fraction background, where criterion 2, by design, typically has
338 higher background mole fractions. The background differences, at a given hour, suggest that the
339 CH₄ field enveloping the city is heterogeneous with differences between towers ranging from 0 to
340 over 20 ppb (Fig. 4g). Because large gradients in CH₄ background over the city could pose
341 challenges for flux estimations using top down methods such as inverse modeling and aircraft mass
342 balance, it is imperative to establish whether the background differences vary randomly or
343 systematically and how to choose a background to minimize these errors.

344 To further understand the nature of background variability we calculate the mean and
345 standard error of background hourly differences over November 2014 to December 2016 for each
346 of the eight wind directions mentioned in Table 1. The results are shown in Fig. 5. Systematic
347 bias is evident for the SE, S, SW, W, and NW wind sectors, whereas random error dominates N,



348 NE, and E wind directions. Wind directions showing bias have mean biases ranging from 2 to 5
349 ppb, with values as large as 8 ppb falling within the range of two times the standard error.

350 Random errors in the mole fractions of background differences are also important and are
351 a function of the length of the data record. We quantify the random error in the CH₄ background
352 mole fraction differences using the bootstrap method by randomly sampling 2 to 150 hours of the
353 background CH₄ differences for each of the wind directions with replacement (we make the
354 assumption that our differences are independent since we eliminated lag 1 autocorrelation from
355 the data). This sub-sampling experiment is repeated 5000 times (Efron and Tibshirani, 1986). The
356 standard deviations of the mean (standard error) of the 5000 simulated differences are calculated
357 for each wind direction. The resulting standard errors of the city CH₄ background, multiplied by
358 2 to represent the 95% confidence intervals, are shown as a function of the length of the data record
359 in Fig. 6. All wind directions demonstrate that, as expected, the random error falls as the sample
360 size grows. In general, 25 hourly samples of data reduce random errors by about 70%. Using less
361 than 25 hourly samples to estimate emissions may result in random errors of CH₄ mole fractions
362 of 5 to 35 ppb. Now we consider these random and systematic errors in the CH₄ background in
363 context of Indianapolis urban CH₄ emissions.

364 For Indianapolis, using INFLUX tower network, we estimated that depending on sample
365 size (number of hours sampled) and wind direction systematic and random errors of CH₄
366 background gradient across the city over 12-16 LST could vary from 0 to 5 ppb and from 5 to 35
367 ppb respectively. Given that the average afternoon CH₄ enhancement of the city is around 8-12
368 ppb (section 3.3; Fig. 7; Cambaliza et al., 2015; Miles et al., 2017), the error on the estimated
369 emissions could be over 100% if the analysis does not approach the issue of background with
370 enough sampling. For CH₄ sources with a significantly larger signal than their regional



371 background, the mentioned background variability becomes less impactful on results, but because
372 Indianapolis is a relatively small emitter of CH₄, the uncertainties due to background are
373 comparatively large. Our random error assessment suggests that the highly variable CH₄ emission
374 values of Indianapolis from the aircraft mass balance calculations (Fig. 1) are at least partially due
375 to the variability in the urban CH₄ background of Indianapolis.

376

377 3.3. Temporal Variability

378 Fig. 7 presents average CH₄ mole fraction enhancements and flux calculations (equation
379 4) at towers 8 and 13 for years 2014, 2016, and 2013-2016 (for the detailed methodology see
380 sections 2.6). The years of 2014 and 2016 are chosen for temporal comparison because they do
381 not contain major BLH data gaps. The error bars in the figure show the standard error multiplied
382 by 2 indicating 95% confidence interval of each average.

383 One of the more interesting features in the Fig. 7 is a day/night variability of CH₄ emissions
384 at Indianapolis. The most prominent example of this feature is found in Fig. 7c, where the
385 estimates for both years suggest that daytime emissions are at least twice as high as the emissions
386 at night. The decrease of the CH₄ emissions at night also appears in tower 13, but the errors are
387 too high in those estimates to make any definitive conclusions. A similar urban CH₄ emissions
388 diurnal variability is reported by Helfter et al. (2016) in their study of GHGs for London, UK,
389 where they attribute diurnal variation of the CH₄ emissions to the NG distribution network
390 activities, fugitive emissions from NG appliances, and to temperature-sensitive CH₄ emission
391 sources of biogenic origin (such as a landfill). Taylor et al. (2018) suggest that CH₄ emissions
392 from landfills exhibit a diurnal cycle with higher emissions in early afternoon and 30-40% lower
393 emissions at night.



394 With regard to yearly temporal variability we are only able to compare years 2014 and
395 2016 due to limited BLH data for other years. Results from both towers suggest that Indianapolis
396 CH₄ emissions did not change significantly.

397

398 **3.4 Sources**

399 Bottom-up emission inventories have difficulty tracking changes in sources over time. Our
400 continuous tower network observations can monitor temporal and spatial variability in sources of
401 CH₄ in Indianapolis. To do so we employ the aforementioned bivariate polar plots to verify known
402 sources and potentially identify unknown sources across the city. We compare two time periods,
403 2014-2015 (two full years) and 2016. Fig. 8 displays bivariate polar plots of CH₄ enhancements
404 using criterion 1 background at 9 INFLUX towers in Indianapolis over the two years of 2014 and
405 2015. Fig. 9 shows the same plot, but for the year 2016. Here we have separated 2016 from 2014-
406 2015 because of different results noted during this time.

407 The images reveal that the most consistent and strongest source in the city is the SSLF.
408 This is most evident from the 40+ ppb CH₄ enhancements detected at towers 7, 10 and 11 coming
409 from the location of the SSLF (by triangulation). Enhancements from the landfill appear to also
410 be detectable at towers 2, 4, 5, and 13. Based on these observations it can be concluded that there
411 is no other source in Marion County comparable in strength to the SSLF. A small fraction of the
412 SSLF plume is likely due to the co-located wastewater facility, but the inventory estimates suggest
413 that the wastewater treatment facility is responsible for no more than 7% of this plume (Cambaliza
414 et al., 2015; Massakkers et al., 2016). The PEP, located in the northwestern section of the city,
415 may be partially responsible for a plume of 5-10 ppb at towers 5 and 11. However, the plume is
416 less detectable using the criterion 2 background value that has higher background (using tower 8



417 as a background) from NW wind direction (not shown), adding uncertainty to the true magnitude
418 of the enhancement from this source. The same is true for towers 2 and 13, which have pronounced
419 plumes when winds are from the NW with the criterion 1 background, but when background 2 is
420 used these plumes vanish (not shown). Such inconsistency makes it difficult to attribute these
421 plumes to an urban source.

422 Another important point is the cluster of large enhancements surrounding tower 10 in 2014
423 - 2015. Because no other tower sees these enhancements (at least at comparable magnitudes), we
424 believe that these plumes are the result of local NG leaks likely from residential sector of
425 Indianapolis. These plumes are not consistent temporally or spatially as they mostly disappear in
426 2016, potentially indicating that they are transient NG distribution leaks. It is reasonable to
427 hypothesize that NG related CH₄ is being emitted by diffuse, small leaks all across the city.
428 However, towers downwind of the city do not see a large or distinct enhancement from the city,
429 especially when compared to the SSLF source. Thus, the diffuse NG source suspected to be twice
430 as large as the SSLF source (Lamb et al., 2016) does not appear to be supported by these data.
431 This finding contradicts conclusions made by Cambaliza et al., (2015), who attributed most of the
432 CH₄ emitted by Indianapolis to NG related activities. We hypothesize that the relatively high
433 Indianapolis CH₄ emissions (see Fig. 1) reported by Cambaliza et al., (2015) are the result of the
434 low sample size of airborne flux estimates, which is prone to large random errors (see section 3.2).
435 Our results indicate that the main CH₄ source in the city is SSLF and that other sources potentially
436 associated with NG distribution are difficult to identify with clarity. This conclusion is in
437 agreement with EPA 2012 inventory (section 2.3).

438

439 **4 Conclusions**



440 We have examined four specific contributions to discrepancies between urban top-down and
441 bottom-up CH₄ emission estimates from Indianapolis; domain definition, heterogeneous
442 background mole fractions, temporal variability in emissions, and source knowledge. Results
443 indicate that the urban domain definition is crucial for the comparison of the emission estimates
444 among various methods. Atmospheric inverse flux estimates for Marion County, which is similar
445 to the domain that is analyzed by inventory and airborne mass balance methodologies (Mays et
446 al., 2009, Cambaliza et al., 2014, Lamb et al., 2016), is 107 mol/s compared to 160 mol/s that is
447 estimated for the larger domain (Hestia inventory domain). This partially explains higher
448 emissions in inverse modeling estimates shown by Lamb et al., (2016); however, 107 mol/s is still
449 about 40-50% higher than what EPA and Lamb et al., (2016) find in their inventories (Fig. 1).

450 The midday Indianapolis atmospheric CH₄ mole fraction background is shown to be
451 heterogeneous with 2-5 ppb, statistically significant biases for NW, W, SW, S and SE wind
452 directions. We focus on midday atmospheric conditions to avoid the complexities of vertical
453 stratification in the stable boundary layer. Background random error is a function of sample size
454 and decreases as a number of independent samples increase. Low sample volumes, such as a few
455 hours of data from a single location, are prone to random errors on the order of 10-20 ppb in the
456 CH₄ enhancement, similar to the magnitude of the total enhancement from the city of Indianapolis.
457 Longer-term sampling and/or more extensive background sampling is necessary to reduce the
458 random errors. Several days of measurements (e.g. 25 total hours of measurement) would reduce
459 random errors to 3-5 ppb, noticeably smaller than the typical enhancement from Indianapolis
460 emissions. This large random error in the CH₄ background may explain Heimburger et al. (2017)
461 finding of large variability in airborne estimates of Indianapolis CH₄ emissions. Given many



462 samples, the airborne studies converge to an average value of CH₄ flux that is close to inventory
463 estimates for Indianapolis (see Fig. 1).

464 Measurement and analysis strategies can minimize the impacts of these sources of error.
465 Spatially extensive measurement of upwind CH₄ mole fractions are recommended. For towers or
466 other point-based measurements, multiple upwind measurement locations are clearly beneficial.
467 For the aircraft mass balance approach, we recommend an upwind transect be measured, lagged
468 in time if possible, to provide a more complete understanding of the urban background conditions.
469 Complex background conditions might suggest that data from certain days or wind directions
470 should not be used for flux calculation. Finally, a mesoscale atmospheric modeling system
471 informed with the locations of important upwind CH₄ sources can serve as a powerful complement
472 to the atmospheric data (Barkley et al., 2017). Such simulations can guide sampling strategies,
473 and aid in interpretation of data collected with moderately complex background conditions.

474 With regard to temporal variability, no statistically detectable changes in the emission rate
475 were observed when comparing 2014 and 2016 CH₄ emissions. However, a large difference
476 between day and night CH₄ emissions was implied from a simple budget estimate. Night (20-5
477 LST) emissions may be 2 times lower than the emissions during the afternoon (12-16 LST) hours.
478 Because prior estimates of top-down citywide emissions are derived using afternoon-only
479 measurements, overall emissions of Indianapolis may be lower than these studies suggest. This
480 bias may be present in studies performed in other cities as well. Our study suggests that day/night
481 differences in CH₄ emissions must be understood if regional emission estimates are to be
482 calculated correctly. Long-term, tower-based observations are an effective tool for understanding
483 and quantifying multi-year variability in urban emissions.



484 One final point addressed in this study is the location of major CH₄ sources in Indianapolis.
485 Analysis of the INFLUX observation data suggests that inventories for Indianapolis are mostly
486 accurate and that there is likely no evidence of a large, diffuse NG source of CH₄ as implied by
487 Lamb et al., (2016). The only major source in the city is SSLF and it is observed at multiple
488 towers. There is evidence for occasional NG leaks, but they appear localized and limited in their
489 strength.

490 Overall, assessment of the CH₄ emissions at Indianapolis highlights a number of
491 uncertainties that need to be considered in any serious evaluation of urban CH₄ emissions. These
492 uncertainties amplify for Indianapolis since its CH₄ emissions are comparable in magnitude to the
493 regional background flow and as our results show it may be difficult at times to distinguish noise
494 in the background from the actual city emissions signal. The evaluation of larger CH₄ sources may
495 be easier with respect to separating signal from background. However, all of the points raised in
496 this work will be nonetheless relevant and need to be addressed for our understanding of urban
497 CH₄ emissions to significantly improve.

498

499 **Author Contribution**

500 Nikolay Balashov, Kenneth Davis, and Natasha Miles developed the study and worked together
501 on generating the main hypothesis of this work. They also wrote most of the manuscript. Nikolay
502 Balashov wrote all of the codes and performed the analyses presented in this work as well as
503 generated all of the figures. Natasha Miles and Scott Richardson helped with maintenance and
504 gathering of the INFLUX tower data. They also wrote section 2.2 of the paper. Thomas Lauvaux
505 helped with the analysis presented in Figure 1 and section 3.1 concerning interpretation of the
506 inversion modeling results from Lamb et al. (2016). Zachary Barkley significantly contributed to



507 discussions regarding the hypothesis and careful presentation of sections 2.6 and 3.3. Timothy
508 Bonin provided all of the lidar data and wrote the second part of section 2.3 regarding the lidar and
509 the methodology used to determine planetary boundary layer heights. He also contributed to
510 sections 2.6 and 3.3.

511

512 **Competing Interests**

513 The authors declare that they have no conflict of interest.

514

515 **Acknowledgements**

516 This research has been supported by the National Institute of Standards and Technology (project
517 number 70NANB10H245). We would like to thank Dr. Bram Maasackers for the helpful
518 discussion regarding the EPA 2012 inventory and the relevant error structure. We also thank Dr.
519 Paul Shepson and Dr. Dennis Lamb for their useful input regarding airborne mass balance flights
520 and the process of compiling an emissions inventory.

521

522

523 **References**

524

525 Alvarez, R. A., Zavala-Araiza, D., Lyon, D. R., Allen, D. T., Barkley, Z. R., Brandt, A. R., Davis,
526 K. J., Herndon, S. C., Jacob, D. J., Karion, A., Kort, E. A., Lamb, B. K., Lauvaux, T.,
527 Maasackers, J. D., Marchese, A. J., Omara, M., Pacala, S. W., Peischl, J., Robinson, A. L.,
528 Shepson, P. B., Sweeney, C., Townsend-Small, A., Wofsy, S. C., and Hamburg, S. P.:
529 Assessment of methane emissions from the U.S. oil and gas supply chain, *Science*,
530 10.1126/science.aar7204, 2018.

531 Arya, S. P.: *Air pollution meteorology and dispersion*, Oxford University Press New York, 1999.

532 Barkley, Z. R., Lauvaux, T., Davis, K. J., Deng, A., Miles, N. L., Richardson, S. J., Cao, Y.,
533 Sweeney, C., Karion, A., Smith, M., Kort, E. A., Schwietzke, S., Murphy, T., Cervone, G.,
534 Martins, D., and Maasackers, J. D.: Quantifying methane emissions from natural gas



- 535 production in north-eastern Pennsylvania, *Atmos. Chem. Phys.*, 17, 13941-13966,
536 10.5194/acp-17-13941-2017, 2017.
- 537 Bakwin, P. S., Tans, P. P., Hurst, D. F., and Zhao, C.: Measurements of carbon dioxide on very
538 tall towers: results of the NOAA/CMDL program, *Tellus*, 50B, 401–415, 1998.
- 539 Bonin, T. A., Carroll, B. J., Hardesty, R. M., Brewer, W. A., Hajny, K., Salmon, O. E., and
540 Shepson, P. B.: Doppler Lidar Observations of the Mixing Height in Indianapolis Using an
541 Automated Composite Fuzzy Logic Approach, *Journal of Atmospheric and Oceanic*
542 *Technology*, 35, 473-490, 10.1175/jtech-d-17-0159.1, 2018.
- 543 Brandt, A. R., Heath, G. A., Kort, E. A., O'Sullivan, F., Pétron, G., Jordaan, S. M., Tans, P.,
544 Wilcox, J., Gopstein, A. M., Arent, D., Wofsy, S., Brown, N. J., Bradley, R., Stucky, G.
545 D., Eardley, D., and Harriss, R.: Methane Leaks from North American Natural Gas
546 Systems, *Science*, 343, 733-735, 10.1126/science.1247045, 2014.
- 547 Cambaliza, M., Shepson, P., Bogner, J., Caulton, D., Stirm, B., Sweeney, C., Montzka, S., Gurney,
548 K., Spokas, K., and Salmon, O.: Quantification and source apportionment of the methane
549 emission flux from the city of Indianapolis, *Elem. Sci. Anth.*, 3, 2015.
- 550 Cambaliza, M. O. L., Shepson, P. B., Caulton, D. R., Stirm, B., Samarov, D., Gurney, K. R.,
551 Turnbull, J., Davis, K. J., Possolo, A., Karion, A., Sweeney, C., Moser, B., Hendricks, A.,
552 Lauvaux, T., Mays, K., Whetstone, J., Huang, J., Razlivanov, I., Miles, N. L., and
553 Richardson, S. J.: Assessment of uncertainties of an aircraft-based mass balance approach
554 for quantifying urban greenhouse gas emissions, *Atmos. Chem. Phys.*, 14, 9029-9050,
555 10.5194/acp-14-9029-2014, 2014.
- 556 Carslaw, D. C., and Ropkins, K.: openair — An R package for air quality data analysis,
557 *Environmental Modelling & Software*, 27-28, 52-61,
558 <https://doi.org/10.1016/j.envsoft.2011.09.008>, 2012.
- 559 Carslaw, D. C., and Beevers, S. D.: Characterising and understanding emission sources using
560 bivariate polar plots and k-means clustering, *Environmental Modelling & Software*, 40,
561 325-329, <https://doi.org/10.1016/j.envsoft.2012.09.005>, 2013.
- 562 Ciais, P., Sabine, C., Bala, G., Bopp, L., Brovkin, V., Canadell, J., Chhabra, A., DeFries, R.,
563 Galloway, J., and Heimann, M.: Carbon and other biogeochemical cycles, in: Working
564 Group I Contribution To The IPCC Fifth Assessment Report. *Climate Change 2013 - The*
565 *Physical Science Basis*, edited by: Stocker, T. F., Qin, D., Plattner, G., Tignor, M., Allen,



- 566 S., Boschung, J., Nauels, A., Xia, Y., Bex, V., and Midgley, P., Cambridge Univ. Press,
567 465-570, 2013.
- 568 Davis, K. J., Deng, A., Lauvaux, T., Miles, N. L., Richardson, S. J., Sarmiento, D. P., Gurney, K.
569 R., Hardesty, R. M., Bonin, T. A., and Brewer, W. A.: The Indianapolis Flux Experiment
570 (INFLUX): A test-bed for developing urban greenhouse gas emission measurements,
571 Elem. Sci. Anth., 5, 2017.
- 572 Deng, A., Lauvaux, T., Davis, K. J., Gaudet, B. J., Miles, N., Richardson, S. J., Wu, K., Sarmiento,
573 D. P., Hardesty, R. M., and Bonin, T. A.: Toward reduced transport errors in a high
574 resolution urban CO₂ inversion system, Elem. Sci. Anth., 5, 2017.
- 575 Efron, B., and Tibshirani, R.: Bootstrap Methods for Standard Errors, Confidence Intervals, and
576 Other Measures of Statistical Accuracy, Statist. Sci., 1, 54-75, 10.1214/ss/1177013815,
577 1986.
- 578 Gurney, K. R., Razlivanov, I., Song, Y., Zhou, Y., Benes, B., and Abdul-Massih, M.:
579 Quantification of Fossil Fuel CO₂ Emissions on the Building/Street Scale for a Large U.S.
580 City, Environmental Science & Technology, 46, 12194-12202, 10.1021/es3011282, 2012.
- 581 Hanna, S. R., Briggs, G. A., and Hosker Jr, R. P.: Handbook on atmospheric diffusion, National
582 Oceanic and Atmospheric Administration, Oak Ridge, TN (USA). Atmospheric
583 Turbulence and Diffusion Lab., 1982.
- 584 Heimbürger, A. M., Harvey, R. M., Shepson, P. B., Stirm, B. H., Gore, C., Turnbull, J., Cambaliza,
585 M. O., Salmon, O. E., Kerlo, A.-E. M., and Lavoie, T. N.: Assessing the optimized
586 precision of the aircraft mass balance method for measurement of urban greenhouse gas
587 emission rates through averaging, Elem. Sci. Anth., 5, 2017.
- 588 Helfter, C., Tremper, A. H., Halios, C. H., Kotthaus, S., Bjorkegren, A., Grimmond, C. S. B.,
589 Barlow, J. F., and Nemitz, E.: Spatial and temporal variability of urban fluxes of methane,
590 carbon monoxide and carbon dioxide above London, UK, Atmos. Chem. Phys., 16, 10543-
591 10557, 10.5194/acp-16-10543-2016, 2016.
- 592 Hendrick, M. F., Ackley, R., Sanaie-Movahed, B., Tang, X., and Phillips, N. G.: Fugitive methane
593 emissions from leak-prone natural gas distribution infrastructure in urban environments,
594 Environmental Pollution, 213, 710-716, <https://doi.org/10.1016/j.envpol.2016.01.094>,
595 2016.



- 596 Hiller, R. V., Neiningner, B., Brunner, D., Gerbig, C., Bretscher, D., Künzle, T., Buchmann, N.,
597 and Eugster, W.: Aircraft-based CH₄ flux estimates for validation of emissions from an
598 agriculturally dominated area in Switzerland, *Journal of Geophysical Research:*
599 *Atmospheres*, 119, 4874-4887, doi:10.1002/2013JD020918, 2014.
- 600 Jackson, R. B., Down, A., Phillips, N. G., Ackley, R. C., Cook, C.W., Plata, D. L., and Zhao, K.
601 G.: Natural gas pipeline leaks across Washington, DC, *Environ. Sci. Technol.*, 48, 2051–
602 2058, doi:10.1021/es404474x, 2014.
- 603 Jeong, S., Millstein, D., and Fischer, M. L.: Spatially Explicit Methane Emissions from Petroleum
604 Production and the Natural Gas System in California, *Environmental Science &*
605 *Technology*, 48, 5982-5990, 10.1021/es4046692, 2014.
- 606 Jeong, S., Newman, S., Zhang, J., Andrews, A. E., Bianco, L., Bagley, J., Cui, X., Graven, H.,
607 Kim, J., Salameh, P., LaFranchi, B. W., Priest, C., Campos-Pineda, M., Novakovskaia, E.,
608 Sloop, C. D., Michelsen, H. A., Bambha, R. P., Weiss, R. F., Keeling, R., and Fischer, M.
609 L.: Estimating methane emissions in California's urban and rural regions using multitower
610 observations, *Journal of Geophysical Research: Atmospheres*, 121, 13,031-013,049,
611 doi:10.1002/2016JD025404, 2016.
- 612 Jeong, S., Cui, X., Blake, D. R., Miller, B., Montzka, S. A., Andrews, A., Guha, A., Martien, P.,
613 Bambha, R. P., LaFranchi, B., Michelsen, H. A., Clements, C. B., Glaize, P., and Fischer,
614 M. L.: Estimating methane emissions from biological and fossil-fuel sources in the San
615 Francisco Bay Area, *Geophysical Research Letters*, 44, 486-495,
616 doi:10.1002/2016GL071794, 2017.
- 617 Kort, E. A., Eluszkiewicz, J., Stephens, B. B., Miller, J. B., Gerbig, C., Nehr Korn, T., Daube, B.
618 C., Kaplan, J. O., Houweling, S., and Wofsy, S. C.: Emissions of CH₄ and N₂O over the
619 United States and Canada based on a receptor-oriented modeling framework and COBRA-
620 NA atmospheric observations, *Geophys. Res. Lett.*, 35, L18808,
621 doi:10.1029/2008GL034031, 2008.
- 622 Lamb, B. K., Cambaliza, M. O. L., Davis, K. J., Edburg, S. L., Ferrara, T. W., Floerchinger, C.,
623 Heimburger, A. M. F., Herndon, S., Lauvaux, T., Lavoie, T., Lyon, D. R., Miles, N.,
624 Prasad, K. R., Richardson, S., Roscioli, J. R., Salmon, O. E., Shepson, P. B., Stirn, B. H.,
625 and Whetstone, J.: Direct and Indirect Measurements and Modeling of Methane Emissions



- 626 in Indianapolis, Indiana, *Environmental Science & Technology*, 50, 8910-8917,
627 10.1021/acs.est.6b01198, 2016.
- 628 Lauvaux, T., Miles, N. L., Deng, A., Richardson, S. J., Cambaliza, M. O., Davis, K. J., Gaudet,
629 B., Gurney, K. R., Huang, J., O'Keefe, D., Song, Y., Karion, A., Oda, T., Patarasuk, R.,
630 Razlivanov, I., Sarmiento, D., Shepson, P., Sweeney, C., Turnbull, J., and Wu, K.: High-
631 resolution atmospheric inversion of urban CO₂ emissions during the dormant season of the
632 Indianapolis Flux Experiment (INFLUX), *Journal of Geophysical Research: Atmospheres*,
633 121, 5213-5236, doi:10.1002/2015JD024473, 2016.
- 634 Maasackers, J. D., Jacob, D. J., Sulprizio, M. P., Turner, A. J., Weitz, M., Wirth, T., Hight, C.,
635 DeFigueiredo, M., Desai, M., Schmeltz, R., Hockstad, L., Bloom, A. A., Bowman, K. W.,
636 Jeong, S., and Fischer, M. L.: Gridded National Inventory of U.S. Methane Emissions,
637 *Environmental Science & Technology*, 50, 13123-13133, 10.1021/acs.est.6b02878, 2016.
- 638 Mays, K. L., Shepson, P. B., Stirm, B. H., Karion, A., Sweeney, C., and Gurney, K. R.: Aircraft-
639 Based Measurements of the Carbon Footprint of Indianapolis, *Environmental Science &*
640 *Technology*, 43, 7816-7823, 10.1021/es901326b, 2009.
- 641 McKain, K., Down, A., Raciti, S. M., Budney, J., Hutyra, L. R., Floerchinger, C., Herndon, S. C.,
642 Nehr Korn, T., Zahniser, M. S., Jackson, R. B., Phillips, N., and Wofsy, S. C.: Methane
643 emissions from natural gas infrastructure and use in the urban region of Boston,
644 Massachusetts, *Proceedings of the National Academy of Sciences*, 112, 1941-1946,
645 10.1073/pnas.1416261112, 2015.
- 646 Miles, N. L., Richardson, S. J., Lauvaux, T., Davis, K. J., Balashov, N. V., Deng, A., Turnbull, J.
647 C., Sweeney, C., Gurney, K. R., and Patarasuk, R.: Quantification of urban atmospheric
648 boundary layer greenhouse gas dry mole fraction enhancements in the dormant season:
649 Results from the Indianapolis Flux Experiment (INFLUX), *Elem. Sci. Anth.*, 5, 2017.
- 650 Miller, S. M., Wofsy, S. C., Michalak, A. M., Kort, E. A., Andrews, A. E., Biraud, S. C.,
651 Dlugokencky, E. J., Eluszkiewicz, J., Fischer, M. L., Janssens-Maenhout, G., Miller, B. R.,
652 Miller, J. B., Montzka, S. A., Nehr Korn, T., and Sweeney, C.: Anthropogenic emissions of
653 methane in the United States, *Proceedings of the National Academy of Sciences*, 110,
654 20018-20022, 10.1073/pnas.1314392110, 2013.
- 655 Myhre, G., Shindell, D., Bréon, F. M., Collins, W., Fuglestedt, J., Huang, J., Koch, D., Lamarque,
656 J. F., Lee, D., Mendoza, B., Nakajima, T., Robock, A., Stephens, G., Takemura, T., and



- 657 Zhang, H.: Anthropogenic and natural radiative forcing, in: Climate Change 2013: The
658 Physical Science Basis. Contribution of Working Group I to the Fifth Assessment Report
659 of the Intergovernmental Panel on Climate Change, edited by: Stocker, T. F., Qin, D.,
660 Plattner, G. K., Tignor, M., Allen, S. K., Doschung, J., Nauels, A., Xia, Y., Bex, V., and
661 Midgley, P. M., Cambridge University Press, Cambridge, UK, 659-740, 2013.
- 662 National Academies of Sciences and Medicine: Improving Characterization of Anthropogenic
663 Methane Emissions in the United States, The National Academies Press, Washington, DC,
664 250 pp., 2018.
- 665 Nisbet, E. G., Dlugokencky, E. J., Manning, M. R., Lowry, D., Fisher, R. E., France, J. L., Michel,
666 S. E., Miller, J. B., White, J. W. C., Vaughn, B., Bousquet, P., Pyle, J. A., Warwick, N. J.,
667 Cain, M., Brownlow, R., Zazzeri, G., Lanoisellé, M., Manning, A. C., Gloor, E., Worthy,
668 D. E. J., Brunke, E.-G., Labuschagne, C., Wolff, E. W., and Ganesan, A. L.: Rising
669 atmospheric methane: 2007–2014 growth and isotopic shift, *Global Biogeochemical*
670 *Cycles*, 30, 1356-1370, doi:10.1002/2016GB005406, 2016.
- 671 Richardson, S. J., Miles, N. L., Davis, K. J., Lauvaux, T., Martins, D. K., Turnbull, J. C., McKain,
672 K., Sweeney, C., and Cambaliza, M. O. L.: Tower measurement network of in-situ CO₂,
673 CH₄, and CO in support of the Indianapolis FLUX (INFLUX) Experiment, *Elem Sci Anth*,
674 5, 2017.
- 675 Sarmiento, D. P., Davis, K. J., Deng, A., Lauvaux, T., Brewer, A., and Hardesty, M.: A
676 comprehensive assessment of land surface-atmosphere interactions in a WRF/Urban
677 modeling system for Indianapolis, IN, *Elem. Sci. Anth.*, 5, 2017.
- 678 Saunio, M., Jackson, R. B., Bousquet, P., Poulter, B., and Canadell, J. G.: The growing role of
679 methane in anthropogenic climate change, *Environmental Research Letters*, 11, 120207,
680 2016.
- 681 Schuh, A. E., Lauvaux, T., West, T. O., Denning, A. S., Davis, K. J., Miles, N., Richardson, S.,
682 Uliasz, M., Lokupitiya, E., Cooley, D., Andrews, A., and Ogle, S.: Evaluating atmospheric
683 CO₂ inversions at multiple scales over a highly inventoried agricultural landscape, *Global*
684 *change biology*, 19, 1424-1439, doi:10.1111/gcb.12141, 2013.
- 685 Taylor, D. M., Chow, F. K., Delkash, M., and Imhoff, P. T.: Atmospheric modeling to assess wind
686 dependence in tracer dilution method measurements of landfill methane emissions, *Waste*
687 *Management*, 73, 197-209, <https://doi.org/10.1016/j.wasman.2017.10.036>, 2018.



- 688 Townsend-Small, A., Tyler, S. C., Pataki, D. E., Xu, X., and Christensen, L. E.: Isotopic
689 measurements of atmospheric methane in Los Angeles, California, USA: Influence of
690 “fugitive” fossil fuel emissions, *J. Geophys. Res.-Atmos.*, 117, 1–11,
691 <https://doi.org/10.1029/2011JD016826>, 2012.
- 692 Turnbull, J. C., Sweeney, C., Karion, A., Newberger, T., Lehman, S. J., Tans, P. P., Davis, K. J.,
693 Lauvaux, T., Miles, N. L., Richardson, S. J., Cambaliza, M. O., Shepson, P. B., Gurney,
694 K., Patarasuk, R., and Razlivanov, I.: Toward quantification and source sector
695 identification of fossil fuel CO₂ emissions from an urban area: Results from the INFLUX
696 experiment, *Journal of Geophysical Research: Atmospheres*, 120, 292-312,
697 doi:10.1002/2014JD022555, 2015.
- 698 Turnbull, J. C., Karion, A., Davis, K. J., Lauvaux, T., Miles, N. L., Richardson, S. J., Sweeney,
699 C., McKain K., Lehman, S. J., Gurney, K., Patarasuk, R., Jianming L., Shepson, P. B.,
700 Heimburger A., Harvey, R., and Whetstone, J.: Synthesis of urban CO₂ emission estimates
701 from multiple methods from the Indianapolis Flux Project (INFLUX), *Environmental
702 Science and Technology*, 53 (1), 287-295, 10.1021/acs.est.8b05552, 2019.
- 703 Van De Wiel, B. J. H. V. d., Moene, A. F., Jonker, H. J. J., Baas, P., Basu, S., Donda, J. M. M.,
704 Sun, J., and Holtslag, A. A. M.: The minimum wind speed for sustainable turbulence in the
705 nocturnal boundary layer, *Journal of the Atmospheric Sciences*, 69, 3116-3127,
706 10.1175/jas-d-12-0107.1, 2012.
- 707 Wunch, D., Wennberg, P. O., Toon, G. C., Keppel-Aleks, G., and Yavin, Y. G.: Emissions of
708 greenhouse gases from a North American megacity, *Geophysical Research Letters*, 36,
709 doi:10.1029/2009GL039825, 2009.
- 710 Zavala-Araiza, D., Lyon, D. R., Alvarez, R. A., Davis, K. J., Harriss, R., Herndon, S. C., Karion,
711 A., Kort, E. A., Lamb, B. K., Lan, X., Marchese, A. J., Pacala, S. W., Robinson, A. L.,
712 Shepson, P. B., Sweeney, C., Talbot, R., Townsend-Small, A., Yacovitch, T. I., Zimmerle,
713 D. J., and Hamburg, S. P.: Reconciling divergent estimates of oil and gas methane
714 emissions, *Proceedings of the National Academy of Sciences*, 112, 15597-15602,
715 10.1073/pnas.1522126112, 2015.
- 716
717
718
719

720 **Tables**

721

722 **Table 1.** INFLUX towers used to estimate CH₄ background based on two different criteria. Numbers in
723 bold indicate towers chosen to generate a background field when multiple options are possible (for more
724 details see discussion). In short, Criterion 1 uses towers with the lowest mean CH₄ for a specific wind
725 direction, and Criterion 2 uses towers not downwind of large sources (including the city as a whole).

Wind Direction	CH ₄ Background Towers	
	Criterion 1	Criterion 2
North (N)	8	13 , 8
Northeast (NE)	8	13 , 8, 2
East (E)	2 , 8	8 , 4, 1, 2
Southeast (SE)	1	8 , 13, 4, 1
South (S)	1	4 , 13, 1
Southwest (SW)	13	1 , 4
West (W)	1	4 , 1
Northwest (NW)	1	8 , 1

726

727

728

729

730

731

732

733

734

735

736

737

738

739

740

741

742

743

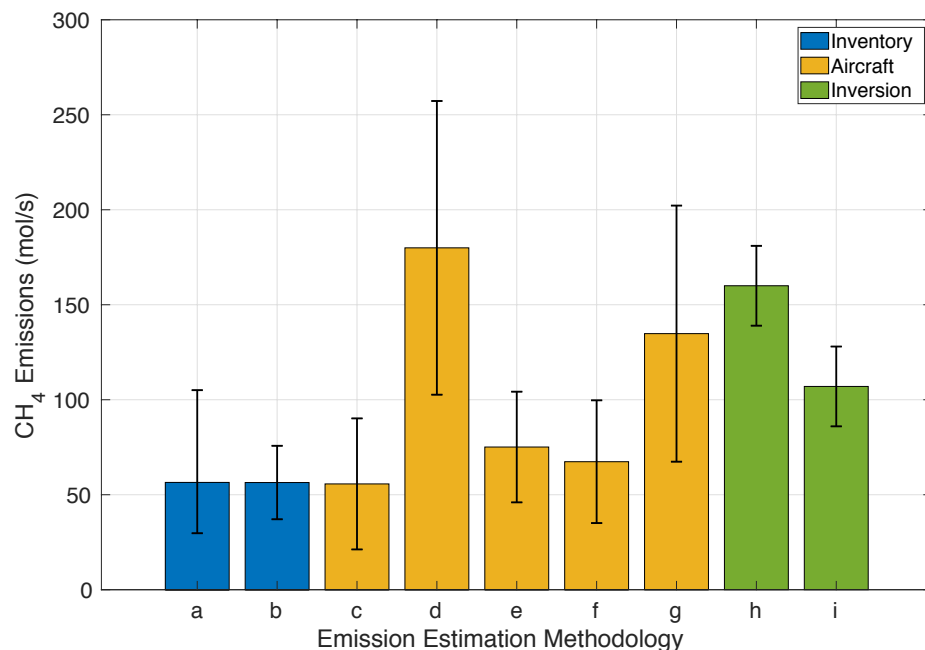
744

745



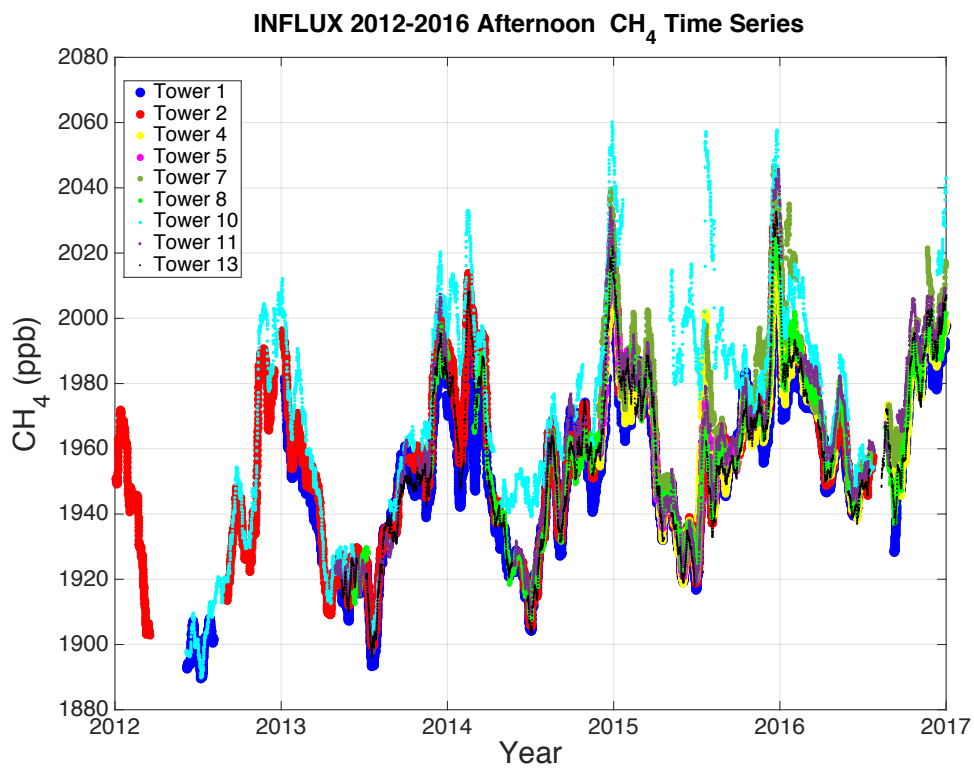
746 **Figures**

747



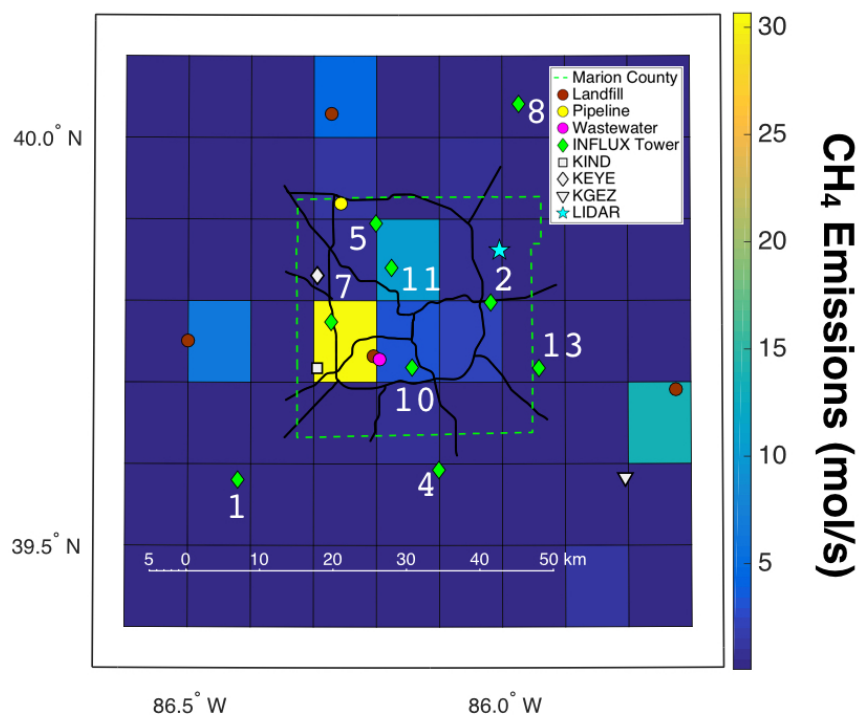
748

749 **Figure 1.** Various estimates of CH₄ emissions at Indianapolis. **(a, b)** Bottom-up estimates of CH₄ emissions
750 conducted by Lamb et al. (2016) in 2013 and Maasackers et al. (2016) based on the EPA 2012 inventory
751 respectively. Error bars show 95% confidence intervals (for more details see above-mentioned articles).
752 **(c-g)** Top-down evaluations of CH₄ emissions with aircraft from various flight campaigns where **(c)**
753 contains 5 flights over March-April of 2008, **(d)** contains 3 flights over November-January of 2008-09, **(e)**
754 contains 5 flights over April-July of 2011, **(f)** contains 9 flights from November-December, 2014, and **(g)**
755 contains the same 5 flights over April-July of 2011 but uses different methodology. Methodologies for **(c-**
756 **f)** are described in Lamb et al. (2016) and methodology for **(g)** is described in Cambaliza et al. (2015).
757 Error bars show 95% confidence intervals (for more details see above-mentioned articles). **(h, i)** Top-down
758 evaluations of CH₄ emissions for 2012-2013 using tower inversion modeling methodology with two
759 different domains, where **(h)** uses the full domain of Fig. 3 and **(i)** uses only the Marion County domain of
760 Fig. 3. The inversion methodology and 95% confidence intervals are described in detail in Lamb et al.
761 (2016).



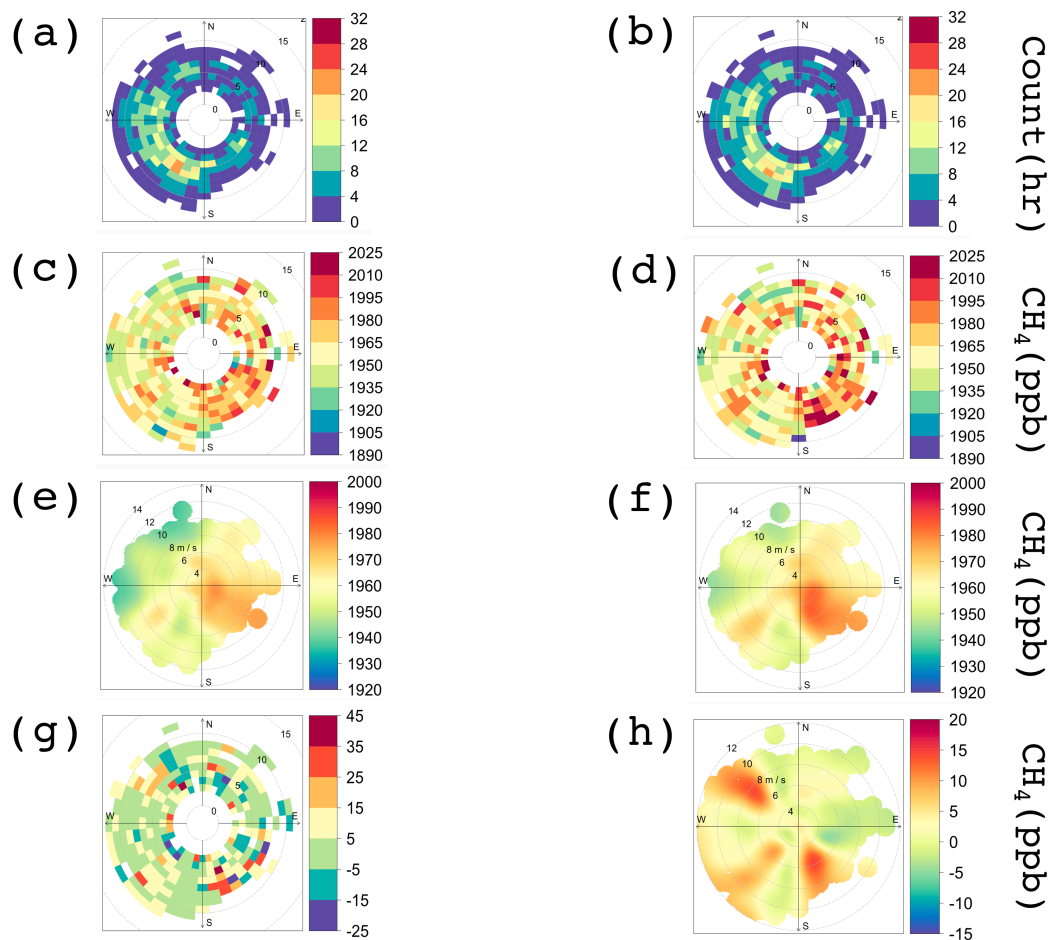
762

763 **Figure 2.** 20-day running average of afternoon (12-16 LST; the hours are inclusive) CH₄ mole fractions
764 as measured by the INFLUX tower network (highest available height is used) from 2012 through 2016.



765

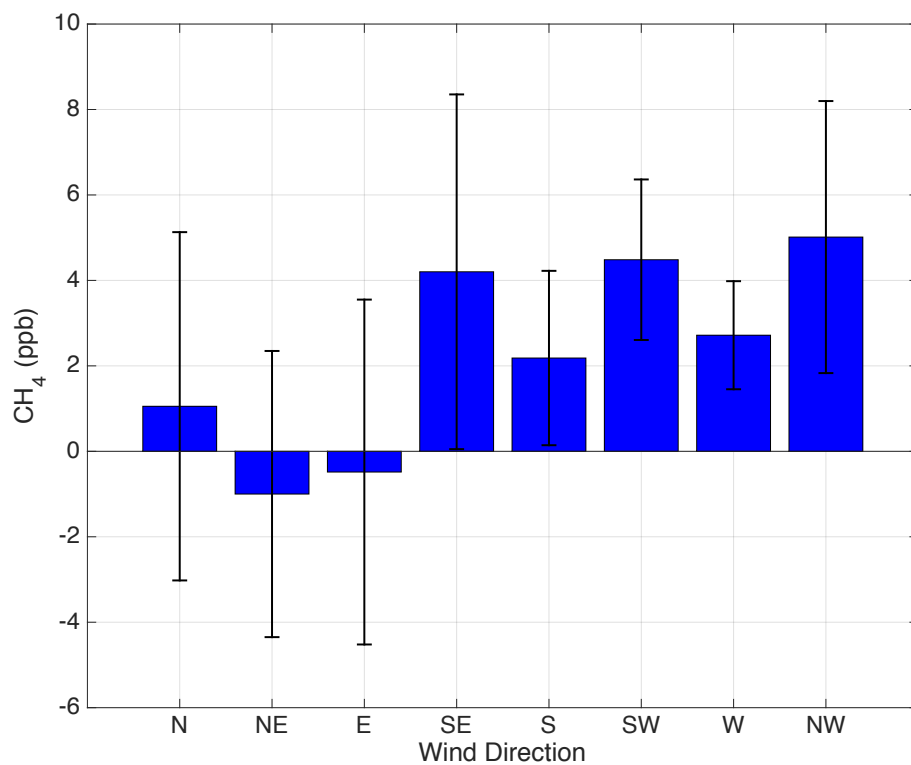
766 **Figure 3.** Map of the primary roads in Indianapolis, INFLUX towers, lidar system, weather stations, and
767 a few CH₄ point sources plotted over the gridded CH₄ emissions (mol/s) from the EPA 2012 Inventory
768 (Maasackers et al., 2016). The gridded map of emissions includes emissions from these point sources; their
769 position is provided to aid in interpretation of the observations. The dashed bright green line denotes
770 Marion County borders.



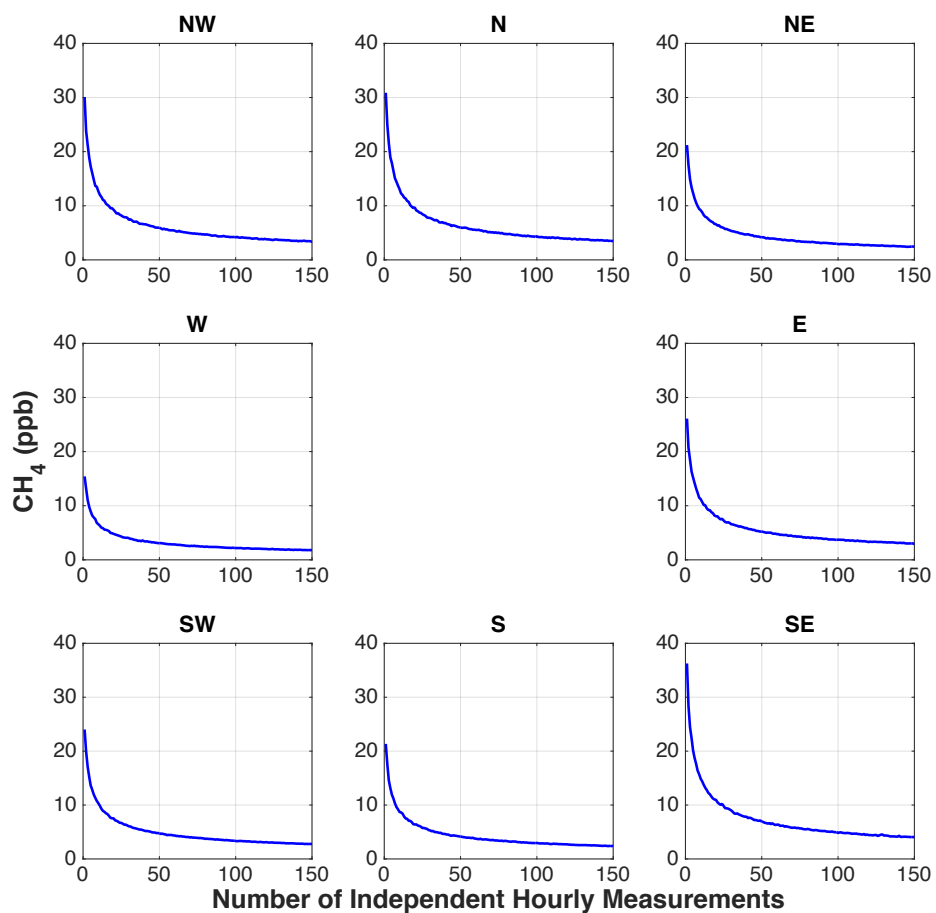
771

772 **Figure 4.** Frequency and bivariate polar plots of CH₄ background for Indianapolis using data from 12-16
 773 LST, and November, 2014 through December, 2016 given 2 different criteria (Table 1). **(a)** Polar histogram
 774 of number of daily measurements available using criterion 1. **(b)** Same as (a) only for criterion 2.
 775 Differences between (a) and (b) are due to slight differences in data availability at the considered towers.
 776 **(c)** Polar frequency plot of the mean CH₄ background using criterion 1. **(d)** Same as (c) only for criterion
 777 2. **(e)** Polar bivariate plot of CH₄ background using criterion 1. **(f)** Same as (e) only for criterion 2. **(g)**
 778 Polar frequency plot of difference between the backgrounds: *criterion 2 – criterion 1*. **(h)** Same as (g)
 779 but shown with a bivariate polar plot.

780



781
782 **Figure 5.** Average of the differences between criteria 2 and 1 CH₄ backgrounds at Indianapolis as a function
783 of wind direction. These averages are generated from the same data as used in Fig. 4 and reflect results
784 shown in Fig. 4g. Error bars indicate standard error × 2.
785



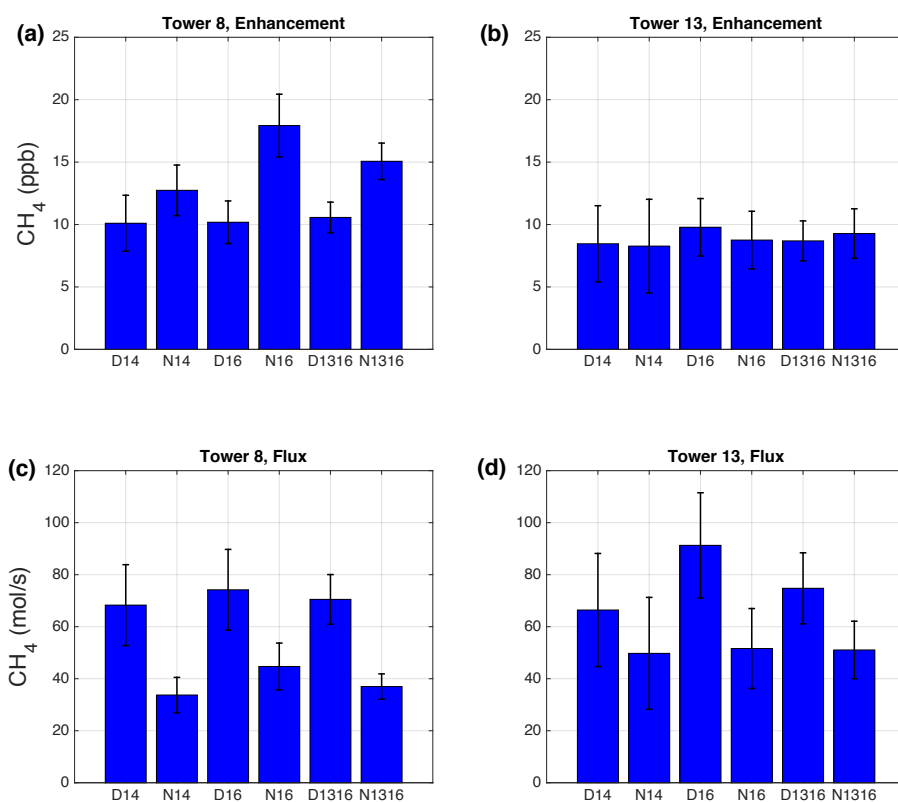
786

787

788

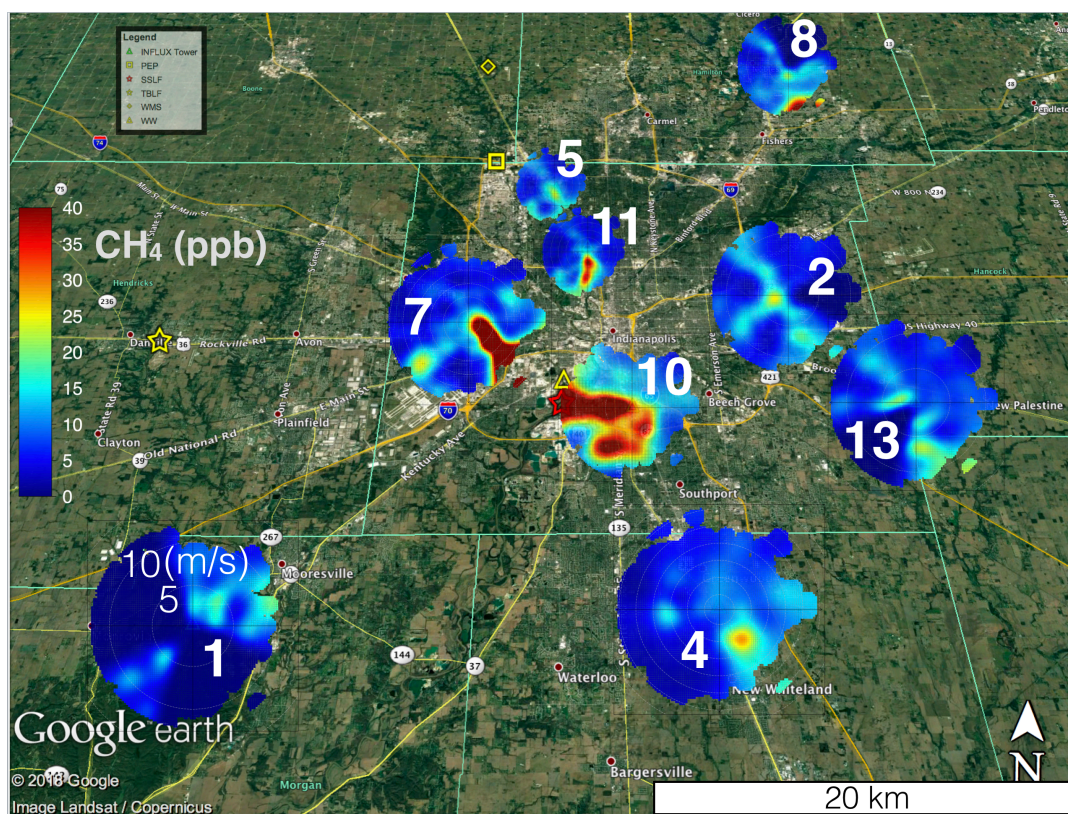
789

Figure 6. Bootstrap simulation of the standard errors multiplied by 2 in Indianapolis CH₄ background mole fraction differences (between criteria 2 and 1) as a function of sample size and wind direction (see text for details).

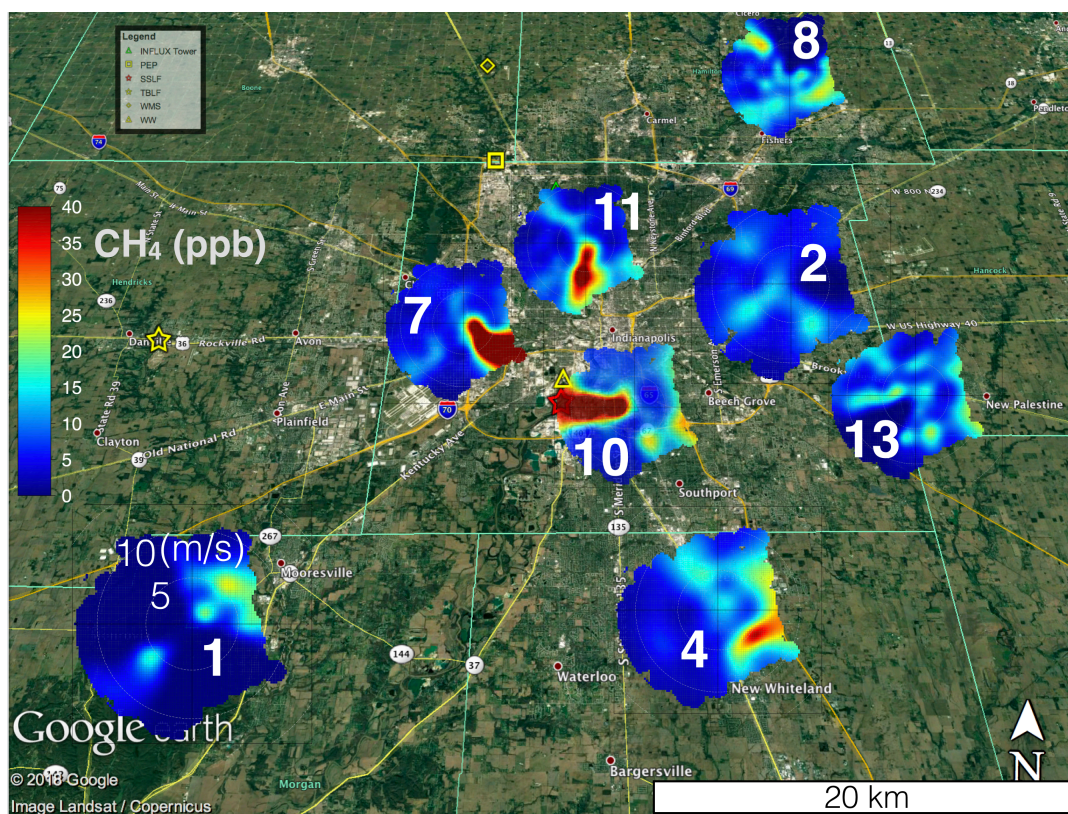


790

791 **Figure 7.** Averages of the daytime (D) and nighttime (N) CH₄ enhancements and fluxes at INFLUX towers
792 8 and 13 for years 2014 (14), 2016 (16), and 2013-2016 (1316). The error bars represent 95% confidence
793 interval of each mean value. (a) Estimates of CH₄ enhancements from tower 8. (b) Estimates of CH₄
794 enhancements from tower 13. (c) Estimates of CH₄ flux from tower 8. (d) Estimates of CH₄ flux from
795 tower 13.



796
797 **Figure 8.** Google Earth image overlaid with bivariate polar plots (section 2.5) of the CH₄ enhancements at
798 9 INFLUX towers in Indianapolis using the criterion 1 background (Table 1) for full years of 2014 and
799 2015 over the afternoon (12-16 LST). The wind speed scale is only labeled at site 1; other sites follow the
800 same convention. Legend indicates known sources of CH₄: Panhandle Eastern Pipeline (PEP), Southern
801 Side Landfill (SSLF), Twin Bridges Landfill (TBLF), Waste Management Solutions (WMS), Waste Water
802 treatment facility (WW). The known magnitudes of sources that are in Marion County (PEP, SSLF, and
803 WW) are reported in section 2.3. Magnitudes of TBLF and WMS according to EPA are approximately 5
804 mol/s. The largest known source on the map is SSLF.



805

806 **Figure 9.** Same as Fig. 8 only for the year of 2016.